AD-A163 308 HILLOCK FORMATION ON (100) GAAS(U) AEROSPACE CORP EL SEGUNDO CA ELECTRONICS RESEARCH LAB S I BOLDISH ET AL. 27 NOV 85 TR-0086(6925-01)-1 SD-TR-85-81 1/1

UNCLASSIFIED F04701-85-C-0086 F/G 20/12 NL

END
FILMED
DTIC

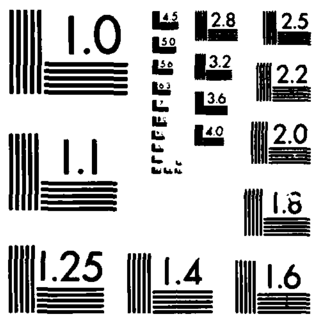

MICROCOPY RESOLUTION TEST CHART
NATIONAL BUREAU OF STANDARDS-1963-A

(12)

REPORT SD-TR-85-81

AD-A163 308

Hillock Formation on (100) GaAs

S. I. BOLDISH
Electronics Research Laboratory

and

P. M. ADAMS
Materials Sciences Laboratory
Laboratory Operations
The Aerospace Corporation
El Segundo, CA 90245

27 November 1985

APPROVED FOR PUBLIC RELEASE;
DISTRIBUTION UNLIMITED

Prepared for

SPACE DIVISION
AIR FORCE SYSTEMS COMMAND
Los Angeles Air Force Station
P. O. Box 92960, Worldway Postal Center
Los Angeles, CA 90009-2960

This report was submitted by The Aerospace Corporation, El Segundo, CA 90245, under Contract No. F04701-85-C-0086 with the Space Division, P.O. Box 92960, Worldway Postal Center, Los Angeles, CA 90009-2960. It was reviewed and approved for The Aerospace Corporation by M. J. Daugherty, Director, Electronics Research Laboratory. Lieutenant Carl Baner, SD/CGX, was the project officer for the Mission-Oriented Investigation and Experimentation (MOIE) program.

This report has been reviewed by the Public Affairs Office (PAS) and is releasable to the National Technical Information Service (NTIS). At NTIS, it will be available to the general public, including foreign nationals.

This technical report has been reviewed and is approved for publication. Publication of this report does not constitute Air Force approval of the report's findings or conclusions. It is published only for the exchange and stimulation of ideas.

CARL BANER, Lt, USAF
Project Officer
SD/CGX

JOSEPH HESS, GM-15
Director, AFSTC West Coast Office
AFSTC/WCO OL-AB

UNCLASSIFIED

SECURITY CLASSIFICATION OF THIS PAGE (When Data Entered)

REPORT DOCUMENTATION PAGE

READ INSTRUCTIONS BEFORE COMPLETING FORM

1. REPORT NUMBER SD-TR-85-81	2. GOVT ACCESSION NO. AD-A163308	3. RECIPIENT'S CATALOG NUMBER
4. TITLE (and Subtitle) HILLOCK FORMATION ON (100) GaAs		5. TYPE OF REPORT & PERIOD COVERED
		6. PERFORMING ORG. REPORT NUMBER TR-0086(6925-01)-1
7. AUTHOR(s) S. I. Boldish and P. M. Adams		8. CONTRACT OR GRANT NUMBER(s) F04701-85-C-0086
9. PERFORMING ORGANIZATION NAME AND ADDRESS The Aerospace Corporation El Segundo, CA 90245		10. PROGRAM ELEMENT, PROJECT, TASK AREA & WORK UNIT NUMBERS
11. CONTROLLING OFFICE NAME AND ADDRESS Space Division Los Angeles Air Force Station Los Angeles, CA 90009-2960		12. REPORT DATE 27 November 1985
		13. NUMBER OF PAGES 17
14. MONITORING AGENCY NAME & ADDRESS(if different from Controlling Office)		15. SECURITY CLASS. (of this report) Unclassified
		15a. DECLASSIFICATION/DOWNGRADING SCHEDULE

16. DISTRIBUTION STATEMENT (of this Report)

Approved for public release; distribution unlimited.

17. DISTRIBUTION STATEMENT (of the abstract entered in Block 20, if different from Report)

18. SUPPLEMENTARY NOTES

19. KEY WORDS (Continue on reverse side if necessary and identify by block number)

GaAs
Gallium arsenide
Hillocks
Surface defects

20. ABSTRACT (Continue on reverse side if necessary and identify by block number)

For application to the growth of gallium arsenide (GaAs) by metal-organic chemical vapor deposition, the dependence of surface morphology and hillock formation on crystal orientation, AsH_3/TMG ratio, and oxide contamination was investigated. Layers of GaAs were deposited on undoped liquid-encapsulated Czochralski (LEC) GaAs substrates oriented either (100) or (100)+2° → <110>. Substrate orientation was checked by Laue X-ray diffraction. Surface features were observed by phase contrast optical microscopy

DD FORM 1473 (FACSIMILE)

UNCLASSIFIED

SECURITY CLASSIFICATION OF THIS PAGE (When Data Entered)

19. KEY WORDS (Continued)

20. ABSTRACT (Continued)

and surface profilometry. To examine the relationship of hillock formation to oxide contamination, GaAs substrate surfaces were exposed to water vapor prior to epitaxial growth. Key [illegible] Gallium Arsenide; Arsenic, Surface [illegible]

CONTENTS

FIGURES

I. INTRODUCTION

Electrical and electro-optical devices fabricated from GaAs grown by metal-organic chemical vapor deposition (MOCVD) must have surfaces and interfaces that are flat and featureless. However, under certain conditions, the MOCVD growth process yields material with "hillocks" on its surface.

Epitaxial GaAs was grown by MOCVD from trimethyl gallium (TMG) and arsine (AsH_3), and conditions of growth were varied to determine the dependence of crystal orientation, AsH_3/TMG ratio, and surface contamination on hillock formation and surface morphology. The MOCVD layers of GaAs were deposited on liquid-encapsulated Czochralski (LEC) GaAs that was undoped and oriented either exactly (100) or (100)+2° → <110>. To verify manufacturer specifications, the orientations of the substrate crystals were checked by X-ray diffraction using the Laue method in the back-reflection mode.

The major defects observed on the surfaces of epitaxial material are *hillocks*, which are commonly found on GaAs grown below 700°C.[1-3] To establish the origin of these defects, water was condensed on the substrate surfaces prior to epitaxial growth, then individual hillocks were profiled by Dek-tak surface profilometry. Water-vapor-exposed GaAs surfaces not used for subsequent MOCVD growth were analyzed by Auger electron spectroscopy.

II. EXPERIMENTAL

The GaAs epitaxial layers were grown at approximately 660°C in a vertical MOCVD reactor chamber at atmospheric pressure. The reactor is 5 cm in diameter, and samples were heated by a resistively powered quartz envelope heater. Hydrogen gas was purified by a palladium diffuser, and the total flow of H_2 gas through the chamber was either 1 or 2.5 standard liters per minute (SLPM). The TMG, from Texas Alkyls, was refrigerated at -10°C; the AsH_3, supplied by Phoenix Research, was a 10% mixture in H_2. The substrates were degreased and chemically etched in a solution of $20NH_4OH:7H_2O_2:485H_2O$ for 30 sec.

The MOCVD system used for this work is unique both because of its heating technique and because the TMG mass flow controller is positioned between the reactor chamber and the TMG bubbler. That positioning allows for the over-pressuring of the TMG bubbler, which enabled the TMG source to be pressure-diluted. In this work a H_2 overpressure of 75 pounds per square inch absolute (PSIA) was used.

In certain experiments, water vapor was deliberately condensed on the GaAs substrates prior to expitaxial growth. Condensation was achieved by heating the top section of the reactor chamber to 170°C in an oven, after which the reactor top was removed from the oven and allowed to cool slightly. The top was then placed on a damp towel so that the towel closed off the mouth of the chamber, and the reactor top with its moist atmosphere was placed over the sample and heater. Within a few seconds, there were fine water droplets on the surface of the GaAs, giving it a fogged appearance. Next, the chamber top was lifted and the droplets evaporated. MOCVD growth procedures were then followed to produce the epitaxial layer, including evacuation of the reactor to 10^{-6} Torr prior to growth.

Water-vapor-coated GaAs samples not used to grow material were analyzed by Auger electron spectroscopy (AES) at SEAL, Inc. A JEOL JAMP-10 scanning Auger microprobe (SAM) was operated in beam brightness mode (BBM) to perform the analysis. With data collected by BBM, we calculated the differential Auger spectrum (see Fig. 6). The BBM technique is implemented by blanking the

primary electron beam so that it periodically reaches the sample. The Auger signal then forms a square wave with time that is recorded by phase-sensitive detection. The result is a highly sensitive and noise-free technique for collecting total counts for an Auger signal.

Samples were prepared for X-ray diffraction analysis by mounting the rough-etched side of a GaAs wafer to a glass slide with low-melting-temperature mounting wax. The back surface of the glass slide was then ground flat and parallel to the front surface of the GaAs wafer. The samples were analyzed by the back-reflection Laue method with unfiltered Cu radiation. Samples were mounted with the wafer surfaces oriented perpendicular to the X-ray beam, and {110} cleavage surfaces were aligned parallel with the sides of the film cassette. Kodak direct exposure film (DEF) recorded the Laue photograph.

III. RESULTS

A. X-RAY DIFFRACTION

Figure 1 displays Laue photographs obtained from the two samples, one from Microwave Associates (Fig. 1a) and the other from Sumitomo Electric (Fig. 1b). The white lines in the Laue photographs are fiducial marks recorded from the film cassette. Given the position and intensity of the Laue spots in the photograph, the Sumitomo Electric wafer (Fig. 1b) displays a well-developed, fourfold symmetry that is consistent with the (100) orientation stated by the manufacturer. On the same basis, the Laue photograph of the Microwave Associates (Fig. 1a) wafer does not exhibit a fourfold symmetry of intensity; however, it does have mirror symmetry at 45° to the fiducial marks on the photograph, which represent <110> axes. Such symmetry indicates that the wafer has been cut and polished several degrees off the (100) axis toward another <110> direction that makes a 45° angle with the (100) axis.

In order to verify the claim made by Microwave Associates that their wafers are cut 2° from (100) toward <110>, the Microwave Associates wafer was rotated 2° away from <110> toward (100) and the (100) Sumitomo Electric wafer was rotated 2° toward <110>. The Sumitomo Electric wafer that was rotated by 2° then produced a Laue photograph (Fig. 1d) almost identical to that of the as-received Microwave Associates sample, whereas the Microwave Associates wafer that was rotated 2° away from <110> toward (100) produced a Laue photograph (Fig. 1c) with good fourfold symmetry and almost identical to the as-received Sumitomo Electric wafer. That a 2° rotation was necessary to transform and produce identical Laue photographs from the Sumitomo Electric and Microwave Associates wafers demonstrates unequivocally that the Microwave Associates wafer is oriented as claimed.

According to SEMI specifications, GaAs wafers are cut 2° toward the nearest <110> direction [(110), $(10\bar{1})$, $(1\bar{1}0)$, (101) in Fig. 2] that cuts the (100) axis at a 45° angle. The Laue photographs provide evidence that Microwave Associates wafers are consistent with this specification. The <110>

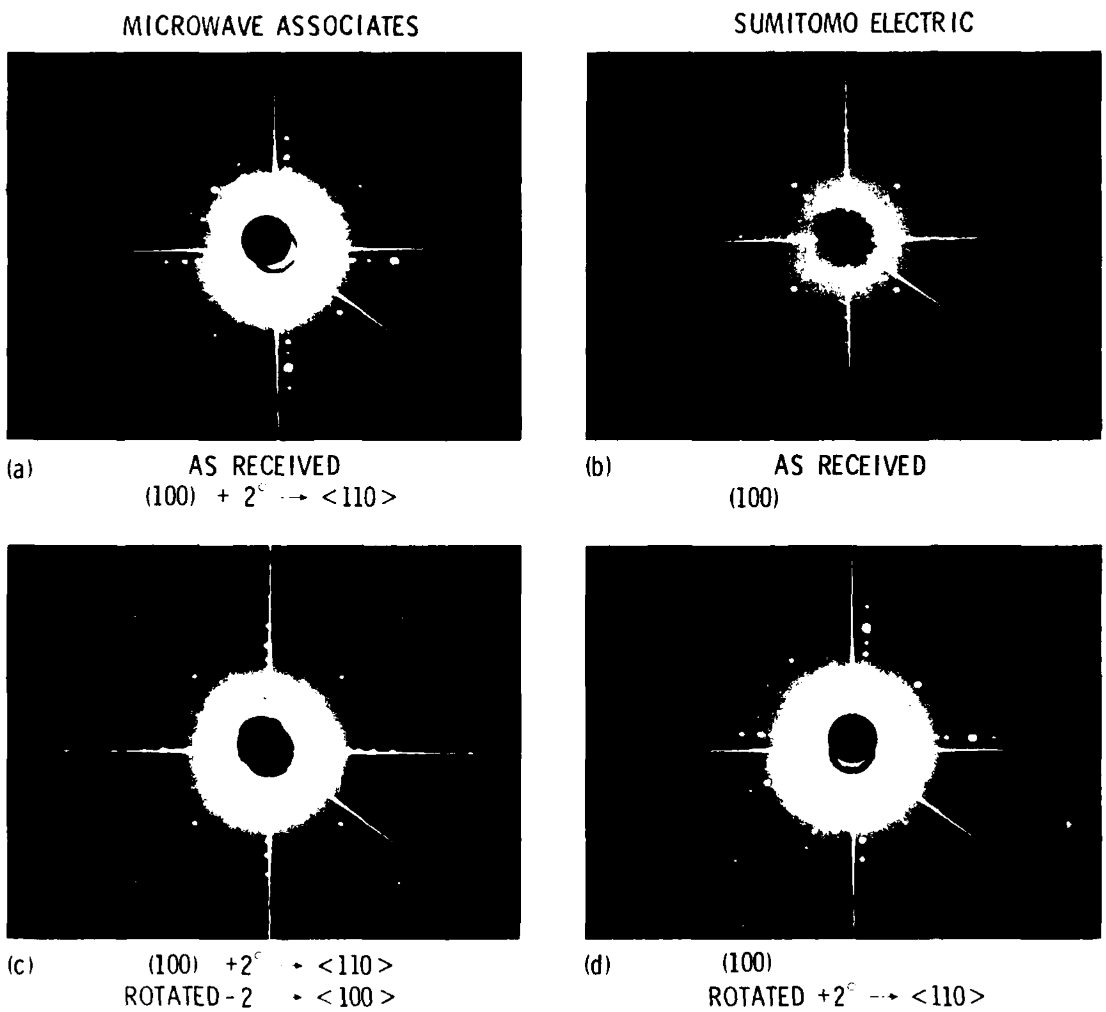

Fig. 1. Back-reflection Laue photographs of GaAs substrates: (a) as-received sample from Microwave Associates, oriented (100)+2° → <110>; (b) as-received sample from Sumitomo Electric oriented (100); (c) Microwave Associates sample rotated -2° toward <100>; (d) Sumitomo Electric sample rotated +2° toward <110>.

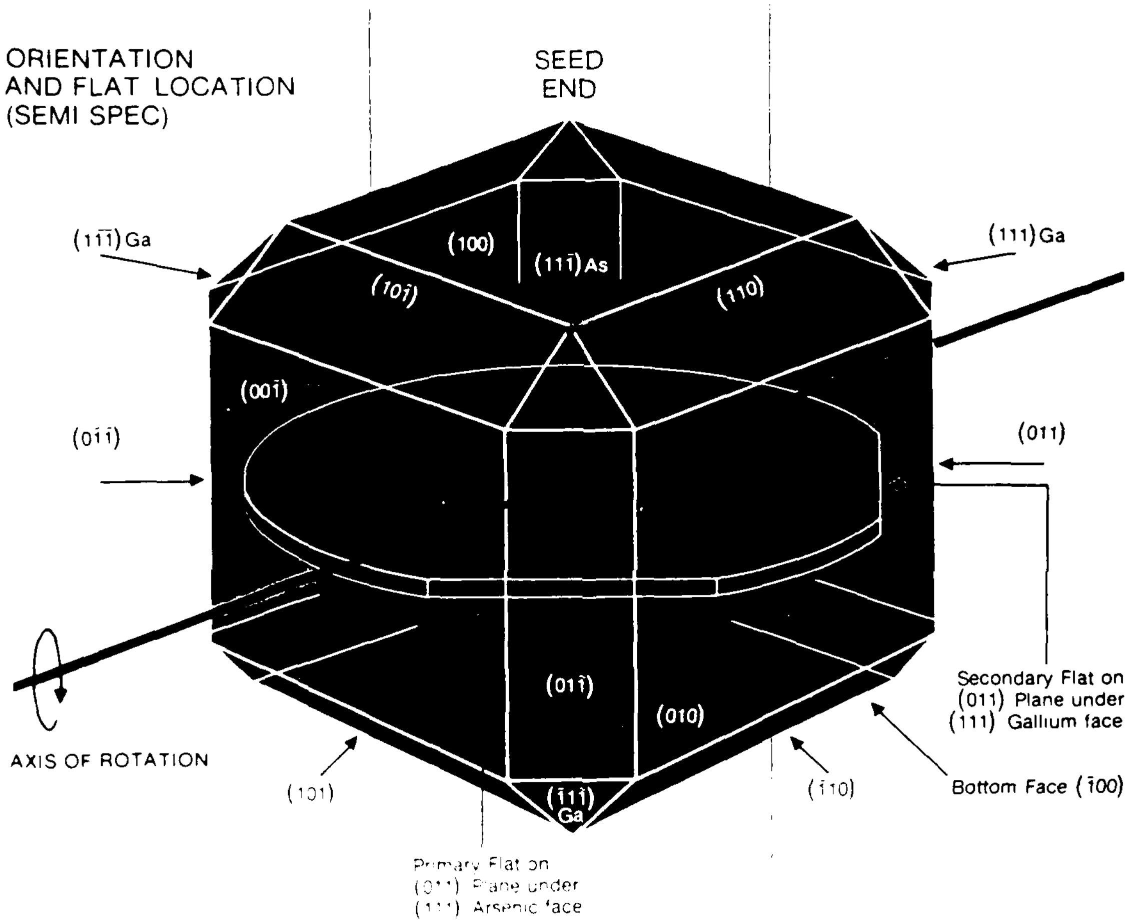

SOURCE: SPECTRUM TECHNOLOGY, INC.

Fig. 2. Crystallographic orientation of lattice planes in gallium arsenide.

cleavage surfaces that were perpendicular with the (100) surface of the wafer [$(0\bar{1}\bar{1})$, $(01\bar{1})$, (011) $(0\bar{1}1)$ in Fig. 2] were aligned so that they would be parallel with the perpendicular fiducial marks on the Laue photograph. The observed misalignment in the Laue photograph (Fig. 1a) was in a direction at 45° to these marks, indicating that the <110> direction of inclination in the wafer was as stated by the manufacturer.

B. MORPHOLOGICAL EFFECTS

Epitaxial layers of GaAs grown with the two substrate orientations had radically different surface morphologies, as Fig. 3 illustrates. Included in the figure is the effect of varying the AsH_3/TMG ratio, where a flow ratio of 15 SCCM/15 SCCM equals a molecular ratio of 9/1. Total flow for these experiments was 1 SLPM. At a low AsH_3/TMG ratio, both orientations yielded poor surface morphologies: hillocks with a three-pointed, funnel-shaped base on the (100)+2° → <110> material; elliptic-cone-shaped defects or hillocks on the (100) substrates. The number of defects for both substrate types decreased with increasing AsH_3/TMG ratio. At the center of the defects is a globule of Ga-rich material. Droplets of Ga may initiate the formation of such hillocks.

A Dek-tak profile across the funnel-shaped growth hillocks (Fig. 4) indicates these defects are actually situated in shallow depressions on the surface of the GaAs. It is almost as if material had been gathered from the surrounding area to build the defect or that the Ga droplet had dissolved material from the surrounding area to form a depression. Yet another explanation is that the depressions are caused by a shadow effect of the defect; that is, the defect blocks material from arriving at the growth surface.

C. H_2O CONDENSATION ON A GaAs SURFACE PRIOR TO GROWTH

The condensation of water vapor prior to epitaxial growth of GaAs on the two types of substrate orientations yielded some interesting results. The most striking effects were those present on the (100)+2° → <110> oriented substrates, illustrated in Fig. 5. With a total flow of H_2 equal to 2.5 SLPM and a flow ratio of AsH_3/TMG equal to 60/15, water vapor effected the growth of many funnel-shaped-base hillocks on the GaAs surface. These defects were

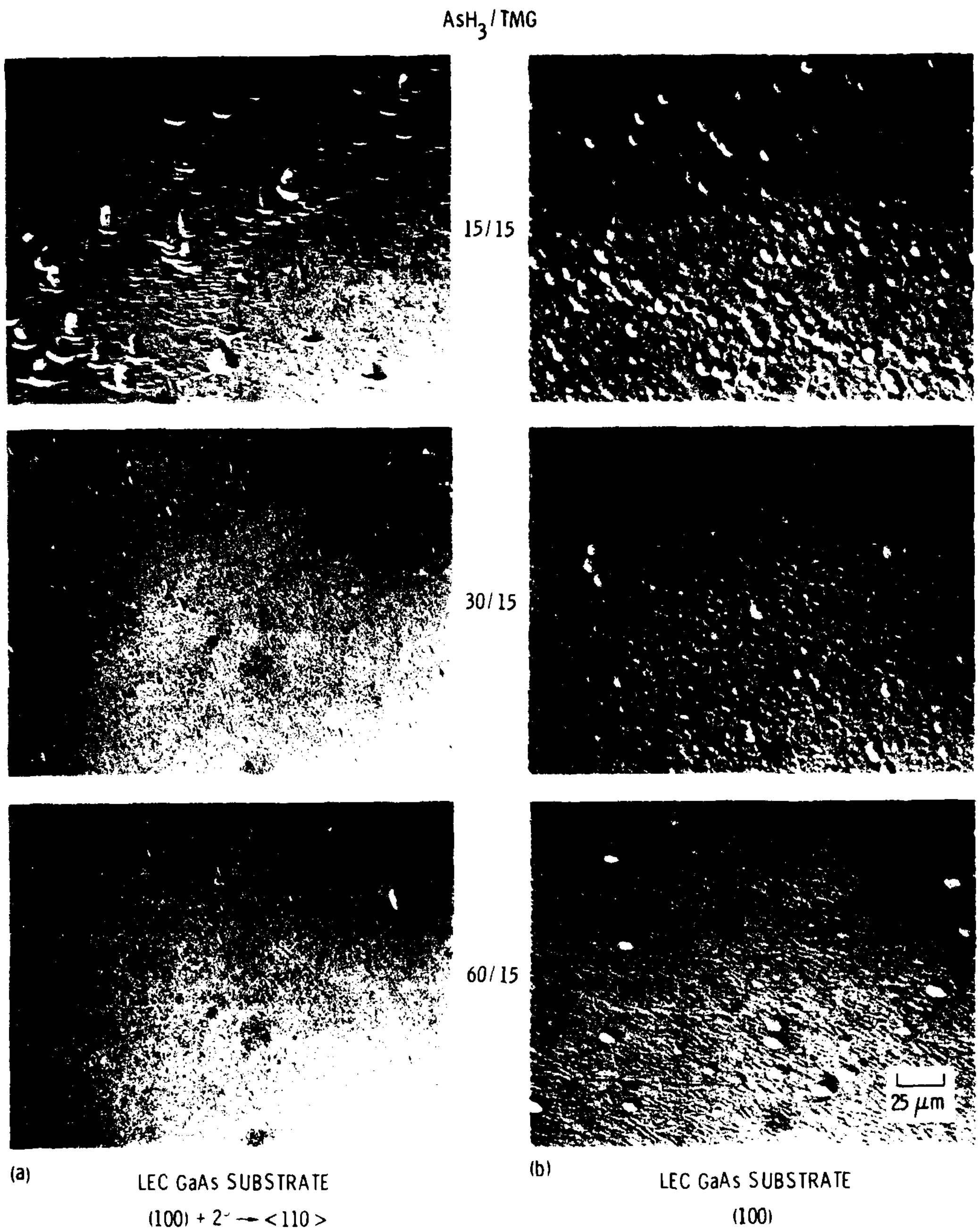

Fig. 3. Surface morphology of MOCVD GaAs as a function of AsH_3/TMG ratio and crystal orientation.

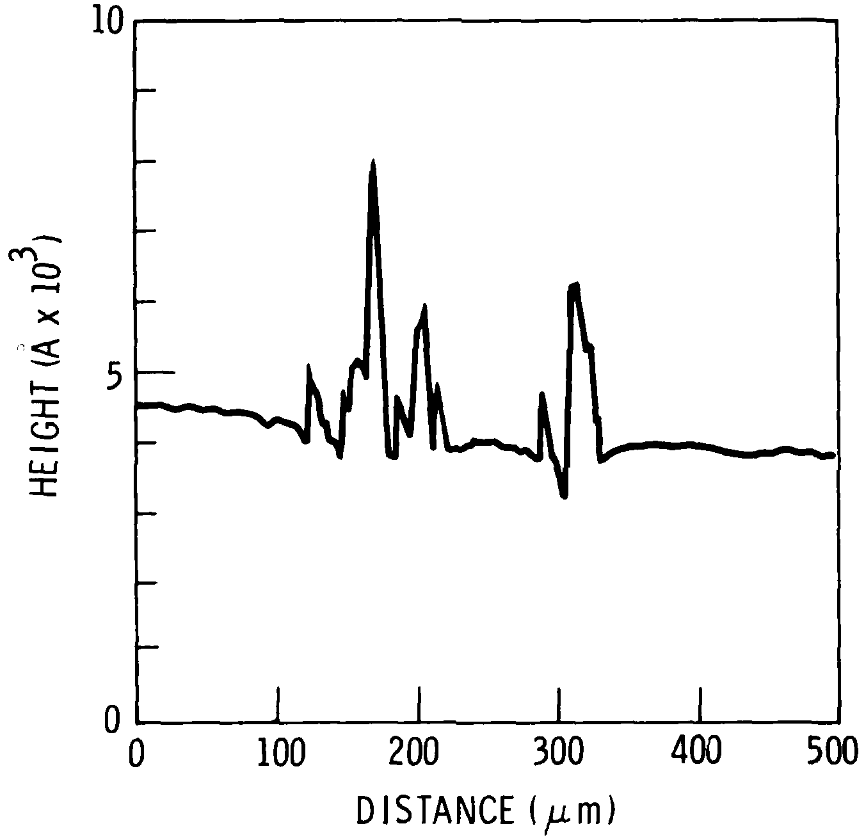

Fig. 4. Dek-tak profile of MOCVD GaAs hillocks with funnel-shaped bases.

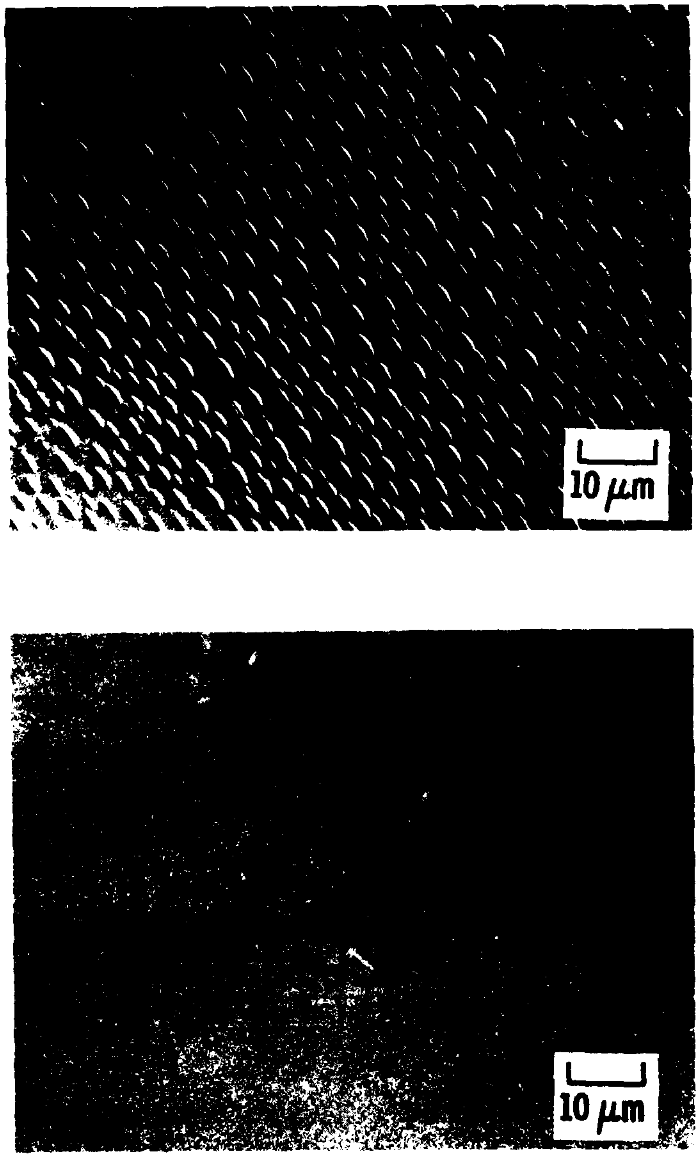

(a)

(b)

Fig. 5. Surface morphology of MOCVD GaAs on (100)+2° → <110> substrates as a function of water-vapor condensation: (a) substrates exposed to water vapor prior to epitaxial growth, and (b) under identical growth conditions but substrate not subjected to condensation.

distributed evenly on the entire surface of the substrate (Fig. 5a) but almost entirely disappeared under identical growth conditions when the substrate was not subjected to water condensation (Fig. 5b). These results were reproducible.

Water condensation seems to have no effect on exact (100) surfaces. Elliptic-cone-shaped defects are found on the surface of the (100) GaAs bunched on a small portion of the wafer, the rest of which is mirror smooth and virtually featureless.

One sample with a (100)+2° → <110> orientation that had been exposed to water vapor but not subsequently used for epitaxial growth of GaAs was analyzed chemically by AES. Clearly, water marks had formed where some of the water drops had evaporated, since the Auger analysis (Fig. 6) reveals the existence of particles containing O, As, and Ga. Depth profiles of some of these particles by Ar^+ ion sputtering show that the composition varies from particle to particle and with depth (Fig. 7). Oxygen-containing particles are oxygen rich at the surface but slowly become richer in As and depleted in O with increasing depth. The Ga concentration remains constant with depth but varies from particle to particle. Figure 7a is a depth profile of the GaAs; Fig. 7b is a depth profile of an oxide particle. There is only a small quantity of O in the GaAs because of surface adsorption of O_2 during sputtering. It is also apparent from the Ga and As data for GaAs that the Auger analysis is not truly quantitative. As the depth profile progresses, both Ga and As should be constant and equal to 50%, but what is observed is an increase in the As concentration to above 50% and a decrease in the Ga concentration to below 50%.

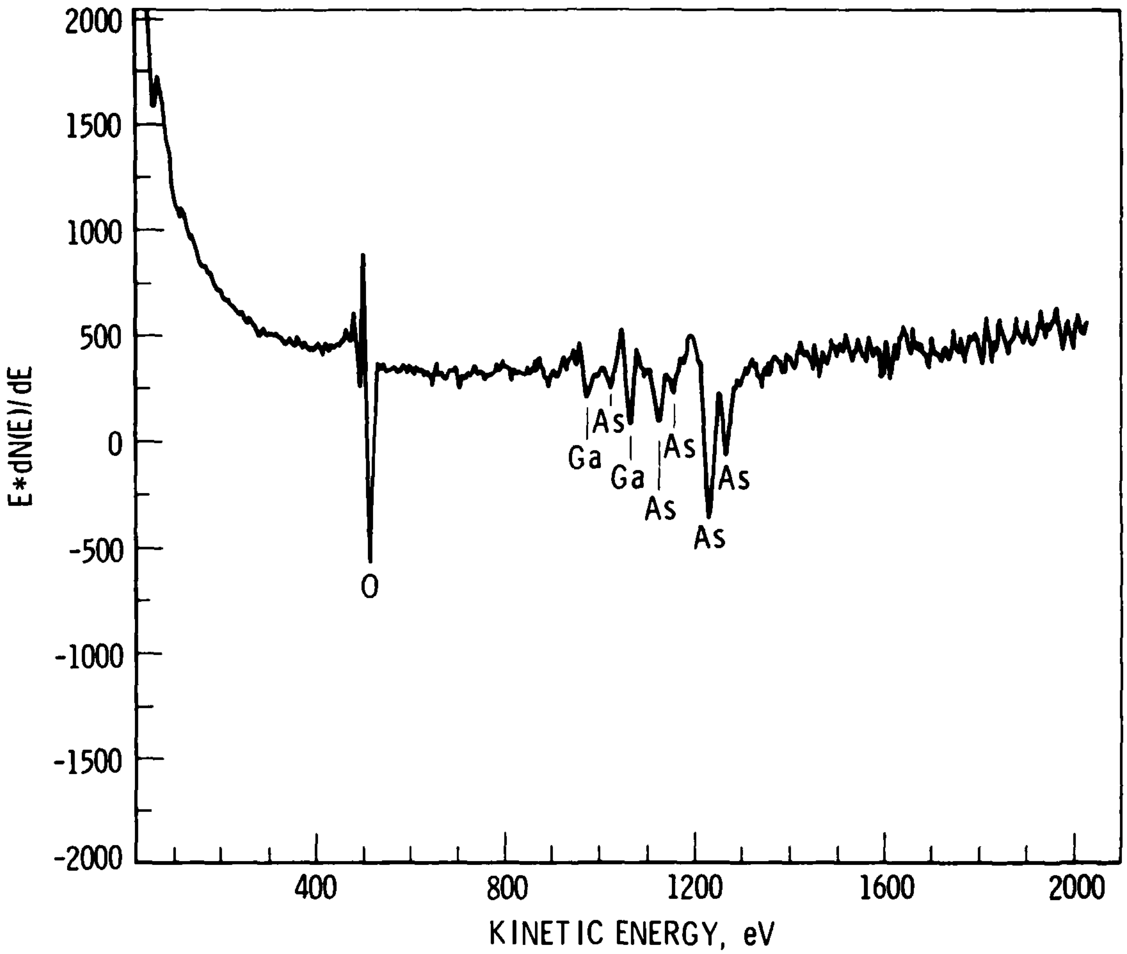

Fig. 6. Auger analysis of (100)+2° → <110> oriented specimen after exposure to water vapor. Water-mark areas contain O, As, and Ga.

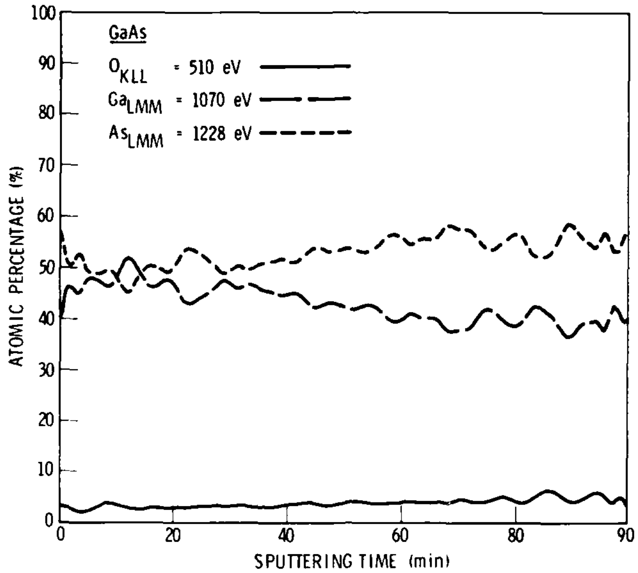

(a)

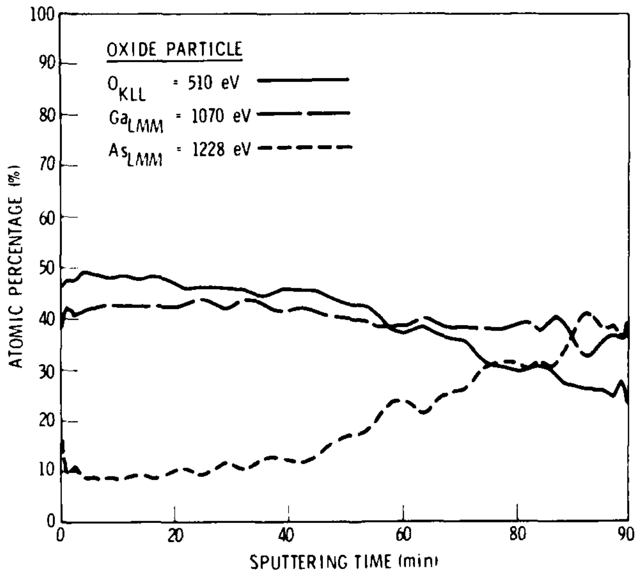

(b)

Fig. 7. Auger depth profile of water-mark sample: (a) GaAs surface; (b) oxide particle.

IV. DISCUSSION

The shape of the hillocks formed in the growth of GaAs by MOCVD depends critically on the orientation of the substrate. (100) oriented substrates yield circular or elliptical defects; (100)+2° → <110> oriented substrates yield triangular (funnel-shaped) defects. Many of the hillocks have a Ga-rich globule at their peak. The number of hillocks decreases for both orientations as the AsH_3/TMG ratio is increased. The observed hillocks are related to the presence of oxides of Ga and As on the GaAs surface of the substrate. This relationship has been demonstrated by the intentional condensation of H_2O vapor and growth of oxides on the GaAs surface prior to epitaxial growth. The formation of oxides by water vapor has been confirmed by Auger analyses of the surfaces of GaAs samples that have been subjected to water vapor. The reduction in the number of hillocks with increasing AsH_3 concentration must be due to the transformation of the oxides to GaAs in the As-rich environment. That these hillocks are reduced in number as the growth temperature increases above 660°C indicates that the oxides of Ga and As are evaporated from the GaAs surface. A direct relationship between the presence of oxides and dislocations and the formation of hillocks cannot be made here. However, Mori and Takagishi[3] have already made a one-to-one association between hillocks and dislocations. Thus, from the work presented here, together with their work, one may infer a relationship between hillocks, dislocations, and the presence of oxides on the GaAs surface.

REFERENCES

1. B. J. Baliga and S. K. Ghandhi, J. Crystal Growth 26, 314 (1974).
2. D. H. Reep and S. K. Ghandhi, J. Crystal Growth 61, 449 (1983).
3. H. Mori and S. Takagishi, J. Crystal Growth 69, 23 (1984).

U.S. GOVERNMENT PRINTING OFFICE: [illegible]

LABORATORY OPERATIONS

The Laboratory Operations of The Aerospace Corporation is conducting experimental and theoretical investigations necessary for the evaluation and application of scientific advances to new military space systems. Versatility and flexibility have been developed to a high degree by the laboratory personnel in dealing with the many problems encountered in the nation's rapidly developing space systems. Expertise in the latest scientific developments is vital to the accomplishment of tasks related to these problems. The laboratories that contribute to this research are:

Aerophysics Laboratory: Launch vehicle and reentry fluid mechanics, heat transfer and flight dynamics; chemical and electric propulsion, propellant chemistry, environmental hazards, trace detection; spacecraft structural mechanics, contamination, thermal and structural control; high temperature thermomechanics, gas kinetics and radiation; cw and pulsed laser development including chemical kinetics, spectroscopy, optical resonators, beam control, atmospheric propagation, laser effects and countermeasures.

Chemistry and Physics Laboratory: Atmospheric chemical reactions, atmospheric optics, light scattering, state-specific chemical reactions and radiation transport in rocket plumes, applied laser spectroscopy, laser chemistry, laser optoelectronics, solar cell physics, battery electrochemistry, space vacuum and radiation effects on materials, lubrication and surface phenomena, thermionic emission, photosensitive materials and detectors, atomic frequency standards, and environmental chemistry.

Electronics Research Laboratory: Microelectronics, GaAs low noise and power devices, semiconductor lasers, electromagnetic and optical propagation phenomena, quantum electronics, laser communications, lidar, and electro-optics; communication sciences, applied electronics, semiconductor crystal and device physics, radiometric imaging; millimeter wave, microwave technology, and RF systems research.

Information Sciences Research Office: Program verification, program translation, performance-sensitive system design, distributed architectures for spaceborne computers, fault-tolerant computer systems, artificial intelligence and microelectronics applications.

Materials Sciences Laboratory: Development of new materials: metal matrix composites, polymers, and new forms of carbon; nondestructive evaluation, component failure analysis and reliability; fracture mechanics and stress corrosion; analysis and evaluation of materials at cryogenic and elevated temperatures as well as in space and enemy-induced environments.

Space Sciences Laboratory: Magnetospheric, auroral and cosmic ray physics, wave-particle interactions, magnetospheric plasma waves; atmospheric and ionospheric physics, density and composition of the upper atmosphere, remote sensing using atmospheric radiation; solar physics, infrared astronomy, infrared signature analysis; effects of solar activity, magnetic storms and nuclear explosions on the earth's atmosphere, ionosphere and magnetosphere; effects of electromagnetic and particulate radiations on space systems; space instrumentation.

END

FILMED

2-86

DTIC